International Journal of Design & Nature and Ecodynamics
Vol. 21, No. 10, October, 2026, pp. 2989-3005
Journal homepage: http://iieta.org/journals/ijdne

2D Electrical Resistivity Tomography for Groundwater Exploration and Borehole Targeting in Al-Haidariya, Najaf, Iraq

Rand Sami[1*], Kadhim Naief Kadhim[1], Amer A. Al-Khalidy[2]

[1] Department of Civil Engineering, University of Babylon, Babylon 51002, Iraq
[2] Department of Applied Geology, College of Science, University of Babylon, Hilla 51002, Iraq

Corresponding Author Email: rand.sami@uobabylon.edu.iq

Copyright: ©2026 The authors. This article is published by IIETA and is licensed under the CC BY 4.0 license (http://creativecommons.org/licenses/by/4.0/).

https://doi.org/10.18280/ijdne.211012

Received: 20 August 2026
Revised: 17 October 2026
Accepted: 24 October 2026
Available online: 31 October 2026

Keywords:
Electrical Resistivity Tomography, groundwater prospecting, RES2DINV, Wenner array, Schlumberger array, Dipole-Dipole array

ABSTRACT

Groundwater is a significant water source in arid and semi-arid areas, especially in regions with growing agricultural and domestic water needs. The purpose of this study is to identify potential groundwater-bearing zones and propose preliminary borehole targets in the Al-Haidariya area of the Najaf Governorate by applying two-dimensional Electrical Resistivity Tomography (ERT). Six ERT profiles were collected using Wenner and Schlumberger arrays, while Dipole-Dipole was employed in five profiles (E1–E3 and E5–E6), excluding E4, with profile lengths of 160 m (for profile E1) and 320 m (for profiles E2–E6). The data collected were processed and inverted using RES2DINV (Version 4.8.10) to generate inverse resistivity sections for subsurface interpretation. The data were interpreted alongside nearby groundwater well data, including static water level (SWL), electrical conductivity (EC), and total dissolved solids (TDS). The measured EC and TDS values ranged from approximately 5.4 to 11.55 mS/cm and 2680 to 5770 ppm, respectively. These relatively high values indicate that groundwater salinity contributes to the low resistivity observed in several ERT sections. Based on the integrated interpretation of the Wenner, Schlumberger and Dipole-Dipole datasets and the results of the neighboring wells, the main preliminary borehole target sectors were identified along E1 at 65–90 m (18–35 m depth), E2 at 90–130 m (18–35 m depth), E3 at 90–130 m (15–35 m depth), E4 at 95–125 m (10–40 m depth), E5 at 210–260 m (20–45 m depth), and E6 at 220–260 m (30–50 m depth), along profiles E1, E2, E3, E4, E5, and E6, respectively. The agreement between the ERT results and the available well data supports the interpretation of the major conductive anomalies as possible potential groundwater-bearing zones, while also suggesting that low resistivity may be influenced by groundwater salinity. The results demonstrate the usefulness of ERT surveys for groundwater potential zone delineation and for minimizing uncertainty in borehole siting in complex subsurface conditions. The proposed drilling targets remain preliminary and require further verification. They can help support preliminary groundwater exploration and borehole targeting, agricultural use, and reduce the economic risks of unsuccessful drilling in water-scarce areas.

1. INTRODUCTION

Groundwater is an important water resource in arid and semi-arid areas where surface water resources are scarce and sensitive to climatic variability and anthropogenic activities. Groundwater is the main source of water for agricultural purposes in the Al-Haidariya area of Najaf Governorate. Due to the lack of reliable information on aquifer distribution and groundwater potential, many drilling attempts have been unsuccessful, resulting in substantial economic losses for local farmers and straining available water resources [1, 2].

Geophysical methods offer an effective and economical alternative to traditional drilling-based investigations for groundwater exploration. Electrical Resistivity Tomography (ERT) is one of the most common techniques for subsurface characterization due to its capability to image lateral and vertical resistivity variations associated with lithology, porosity, moisture content, and groundwater saturation. Low-resistivity zones are typically found in saturated formations, while high-resistivity zones are typically found in dry sediments or possible geological units [3, 4]. ERT is the effective way for identifying water-influenced weak zones and clay-infilled karst features within the overburden, providing clear lateral continuity of these zones along the profiles [5].

Groundwater and subsurface investigations have been successfully conducted in several studies in Iraq using ERT. A two-dimensional Electrical Resistivity Tomography (2D ERT) survey was conducted in the arid area southwest of Samawah City, Al-Muthannā Governorate, southern Iraq, to delineate potential groundwater aquifers. 10 survey lines were acquired using the Wenner–Schlumberger array. The interpreted resistivity models revealed three main subsurface zones. The study showed the effectiveness of 2-D resistivity imaging in discovering groundwater aquifers and distinguishing water-

bearing formations from impermeable geological units [6]. Resistivity data were combined with geological data to delineate groundwater-bearing formations in Babylon [7]. Likewise, the efficiency of ERT for mapping resistivity variations associated with groundwater was demonstrated in western Ramadi [8]. Another study conducted in AL-Najaf City, Iraq, to evaluate subsurface soil conditions as part of foundation investigations by 2D ERT, three electrode arrays were used: Wenner, Schlumberger, and Dipole–Dipole in the survey to locate weak zones, cavities, and changes in soil moisture and lithology. The results showed that using different electrode configurations helps achieve better conditions for subsurface characterization and to make more dependable geotechnical assessments [9]. At the Palm Towers site on the Al-Muthanna Airport land in Baghdad, 2D electrical resistivity imaging was used for subsurface soil investigation; the results identified two main zones: saturated and unsaturated [10]. In Al-Diwaniyah, Iraq, electrical resistivity measurements were used to assess subsurface soil conditions for the design of an electrical power station. The outcomes showed that soil resistivity varies with lithology, moisture content, and engineering properties, which are important factors in grounding-system design and foundation planning. The study demonstrated the value of geoelectrical investigations for optimizing electrical infrastructure projects, ensuring safe and efficient station performance [11].

In contrast, very few hydrogeophysical studies have been carried out in the Al-Haidariya area. The current study uses two-dimensional ERT along six profiles with Wenner, Schlumberger, and Dipole–Dipole arrays, except for profile E4, where Dipole–Dipole measurements were not acquired.

The findings of the present work can support improving sustainable groundwater development and water resource planning in this agricultural study area.

The present work focuses on the Al-Haidariya region as the area under investigation to evaluate groundwater conditions, motivated by the greater demand within the local farming community for sustainable water supplies. The scope of this study is to provide scientifically based information on groundwater occurrence to support agricultural activities and improve water management practices in the region.

Specifically, the scope of this study is to identify potential groundwater-bearing zones and preliminary borehole targets, and to reduce uncertainty in groundwater exploration and assist in the placement of wells for long-term agricultural sustainability in the region through geophysical techniques.

2. STUDY AREA AND GEOLOGICAL–HYDROGEOLOGICAL SETTING

2.1 Location, land use, and accessibility

In Al-Najaf Governorate, the study area is located in the Al-Haidariya District, central Iraq, about 150 km south of the capital, Baghdad, at approximately 32.191° N and 44.068° E (Figure 1). The region is a significant agricultural area with groundwater as the main source of irrigation. Reaching the study area was generally good, supported by main roads and agricultural paths, allowing easier field survey and data acquisition.

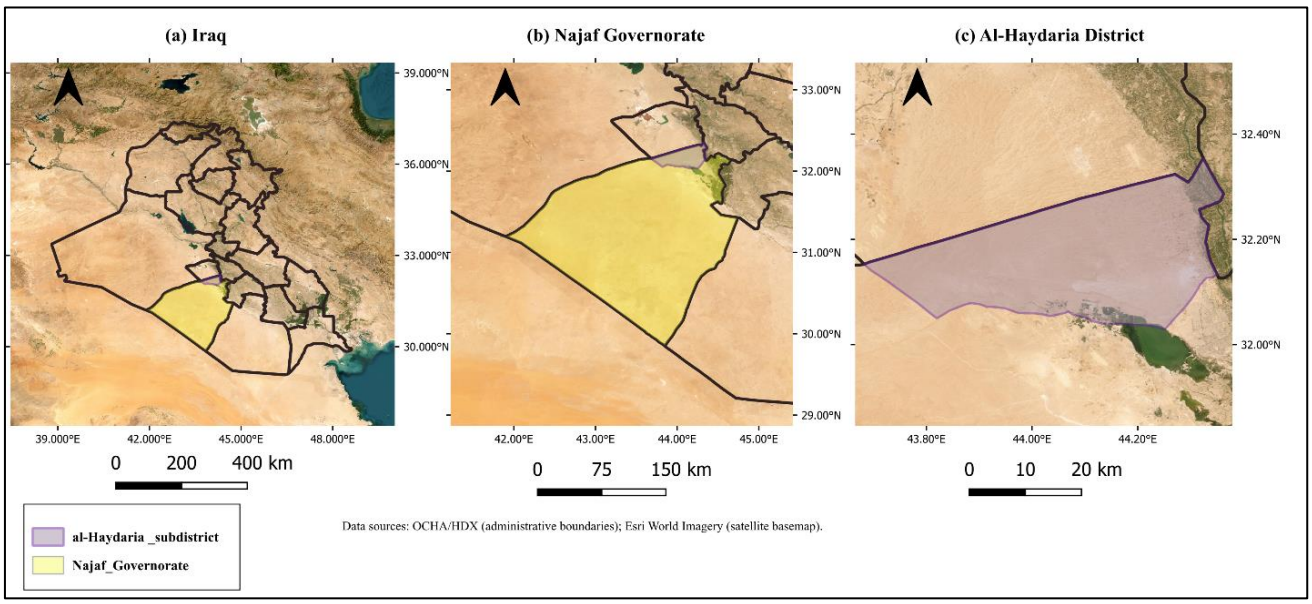

Figure 1. Iraq map showing the study area

2.2 Climate and topography

The area is semi-arid with low annual rainfall and high evaporation rates; groundwater is the primary source of water. This area has low annual rainfall (about 95–135 mm), high temperatures in summer (more than 40 °C), and high evaporation rates, which makes the use of groundwater resources essential for agricultural activities [12]. In general, the topography is flat to gently rippled with little topographic variation. Such conditions are favorable for a geophysical investigation, mainly an electrical resistivity measurement.

2.3 Geological setting

The investigated area lies approximately midway along the Najaf–Karbala Plateau, a geological transition area separating the Stable Shelf and the Mesopotamian Plain within central Iraq. The geological sequence is mainly composed of Neogene to Quaternary deposits, consisting of the Injana, Nfayil, and Dibdibba formations, formed mainly of clastic materials,

covered by alluvial and desert sediments. Changes in Lithology produce differences in subsurface electrical characteristics, providing favorable conditions for electrical resistivity surveys [13].

2.4 Hydrogeological setting and implications for Electrical Resistivity Tomography interpretation

Groundwater mainly occurs within aquifers of Neogene and Quaternary deposits, while permeability and aquifer storage capacity are controlled by lithology. The dry-to-semi-dry climate restricts groundwater recharge, which occurs mainly during seasonal rainfall events. The groundwater flow is generally west to east and north-east in the region. Differences in subsurface lithology may partly explain the resistivity variations observed across the six ERT profiles. The observed conductive zones may be associated with saline groundwater saturation, clay-rich sediments, or both. However, the absence of detailed borehole lithological logs prevents direct correlation of these anomalies with particular geological formations. Therefore, the suggested groundwater-bearing zones, possible hydraulic barriers, and flow pathways remain tentative interpretations rather than confirmed hydrogeological features.

3. MATERIALS AND METHODS

3.1 Electrical Resistivity Tomography survey and inversion

This study employed two-dimensional ERT to investigate potential groundwater-bearing zones. This technique was selected because it provides subsurface information with limited ground disturbance and relatively low investigation costs, making it useful for groundwater exploration in agricultural areas. The ERT method involves injecting electrical current into the ground through two current electrodes and recording the resulting potential difference using two potential electrodes. The apparent resistivity values were computed using Ohm's law and then inverted to get subsurface resistivity distributions [3, 14]. An ABEM Terrameter LS2 multi-electrode system [15] was used to acquire the ERT data, as shown in Figure 2. Six ERT profiles (E1–E6) were obtained, and their spatial distribution is illustrated in Figure 3. Each survey profile consisted of 32 electrodes. Three electrode arrays were used across the study: Wenner, Schlumberger, and Dipole–Dipole. The nominal survey line lengths were 320 m for profiles E2–E6 and 160 m for E1, with electrode spacings of 10 m and 5 m, respectively. The spatial distribution of the ERT survey profiles is illustrated in Figure 3. The configurations available for each profile are summarized in Table A1 (Appendix A).

For profile E4, the Dipole–Dipole survey could not be conducted due to a technical malfunction of the ABEM Terrameter LS2 during field measurements. Therefore, only the Wenner and Schlumberger arrays were available for this profile. All profiles were oriented in a north–west (N-W) direction to ensure adequate spatial coverage of the study area. The Wenner array was selected for its high signal strength and stable data [16], and the Schlumberger array was selected for its greater depth penetration [17]. The Dipole–Dipole array was selected for its ability to detect horizontal resistivity contrasts and resolve localized and vertically oriented subsurface features [18, 19]. The acquired data were processed and inverted in RES2DINV (Version 4.8.10) to create 2-D resistivity models of the subsurface. The inversion process was carried out with the software's existing settings, without manually adjusting the inversion constraints. The Automatically Switch Electrodes option was applied to address electrode-order and geometric-factor sign inconsistencies. All recorded data points were retained before performing the first inversion, without manual removal. Subsequently, the RMS Error Statistics option was used to identify and exclude anomalous measurements showing relatively high misfit between observed and calculated apparent resistivity values. No topographic correction was applied because the survey profiles were located on relatively flat terrain. The inversion results were interpreted according to the association between variations in resistivity, lithological changes, soil moisture content, and groundwater saturation level. Zones of reduced resistivity were considered as potential groundwater-bearing zones for preliminary borehole targeting, subject to further field verification. The inversion errors reported in the results represent the absolute error (Abs. error) values obtained from RES2DINV. For comparative purposes, the inversion models were classified according to their Abs. error values: below 10% as high-quality fits, 10–20% as moderate-quality fits, and above 20% as low-quality fits. These limits were adopted as practical criteria for evaluating inversion data fit rather than as definitive indicators of geological interpretation reliability.



Figure 2. Multi-electrode Electrical Resistivity Tomography (ERT) survey equipment used in the study

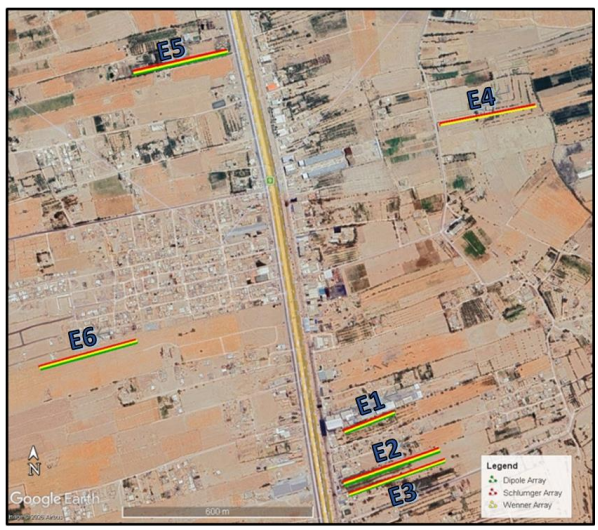

Figure 3. The locations of the Electrical Resistivity Tomography (ERT) survey lines (E1–E6) in the study area

3.2 Groundwater physicochemical field measurements

Field measurements of groundwater quality were performed between April 2025 and February 2026 with a portable multiparameter water quality meter (Model C-600). In the early field surveys, various groundwater quality parameters were measured, including electrical conductivity (EC), total dissolved solids (TDS), pH, salinity, and temperature. During later surveys, measurements were mainly limited to EC and TDS due to their importance in interpreting subsurface electrical resistivity variations. The groundwater physicochemical measurements presented in Tables 1–6 were conducted during field visits between April 2025 and February 2026. However, the exact sampling dates for individual wells were not available; therefore, sampling dates are not provided.

4. RESULTS AND INTERPRETATION

The Wenner, Schlumberger, and Dipole-Dipole configurations were applied to generate the obtained inverted sections to identify possible saturated zones and locate suitable well positions in the selected area. The main inversion parameters and results for the six ERT profiles, including the number of iterations, Abs. error, resistivity ranges, and maximum model depths, are summarized in Table B1 (Appendix B). To facilitate comparison among the six ERT profiles, Table C1 (Appendix C) summarizes the proposed borehole locations and depths, absolute inversion errors, agreement among electrode arrays, and associated interpretation confidence levels.

4.1 Profile E1

From Figure 4, the inverted Wenner model closely matches the measured and calculated data, with an Abs. error of 3.6%. The section presents a clear zone of low resistivity between about 50 and 100 m along the survey line. In this anomaly, the resistivity locally decreases to less than 1 Ω·m and reaches depths exceeding 20 m. This conductive body may be considered a potential groundwater-bearing zone. The resistivity contrast between 50 and 75 m may be a boundary between rock formations or a groundwater accumulation zone.

In Figure 5, the resulting data are well represented by the Schlumberger inversion model, with an Abs. error of 6.5%. The section shows a region of low resistivity from 30 to 105 m along the profile and from 14 to a depth greater than 30 m. Resistivity in these zones is generally less than 3 Ω·m, given the presence of a possible groundwater-bearing zone. A small conductive feature at ~80 m along the profile may indicate a potentially saturated zone.

The Dipole–Dipole section shown in Figure 6 exhibits lateral variations in subsurface resistivity. A wide low-resistivity anomaly begins at the first part of the profile and extends to approximately 100 m, especially at deeper depths, whereas higher resistivity values dominate the interval between about 100 and 125 m close to the profile end. The low-resistivity area could reflect saturated or saline materials, while the resistive area may indicate dry and coarse sediments. With an Abs. error of 28.9%, the interpretation is mainly based on the main resistivity structures instead of minor resistivity variations.

The three arrays show a similar low-resistivity anomaly predominantly within the 55–100 m interval within the ERT line, especially below about 12m. Within the Wenner and Schlumberger models, this zone displays resistivity values ranging from about 1.1 to 5.8 Ω·m in the Wenner array, whereas the Schlumberger result reveals values within a similar range of about 1.3–7.9 Ω·m. The Dipole–Dipole model also exhibits an area of low resistivity within nearly the same interval, showing values ranging from about 0.5 to 6.3 Ω·m. These conductive features could reflect potential groundwater-bearing formations, mainly where the conductive zones show good continuity and appear in more than one array.

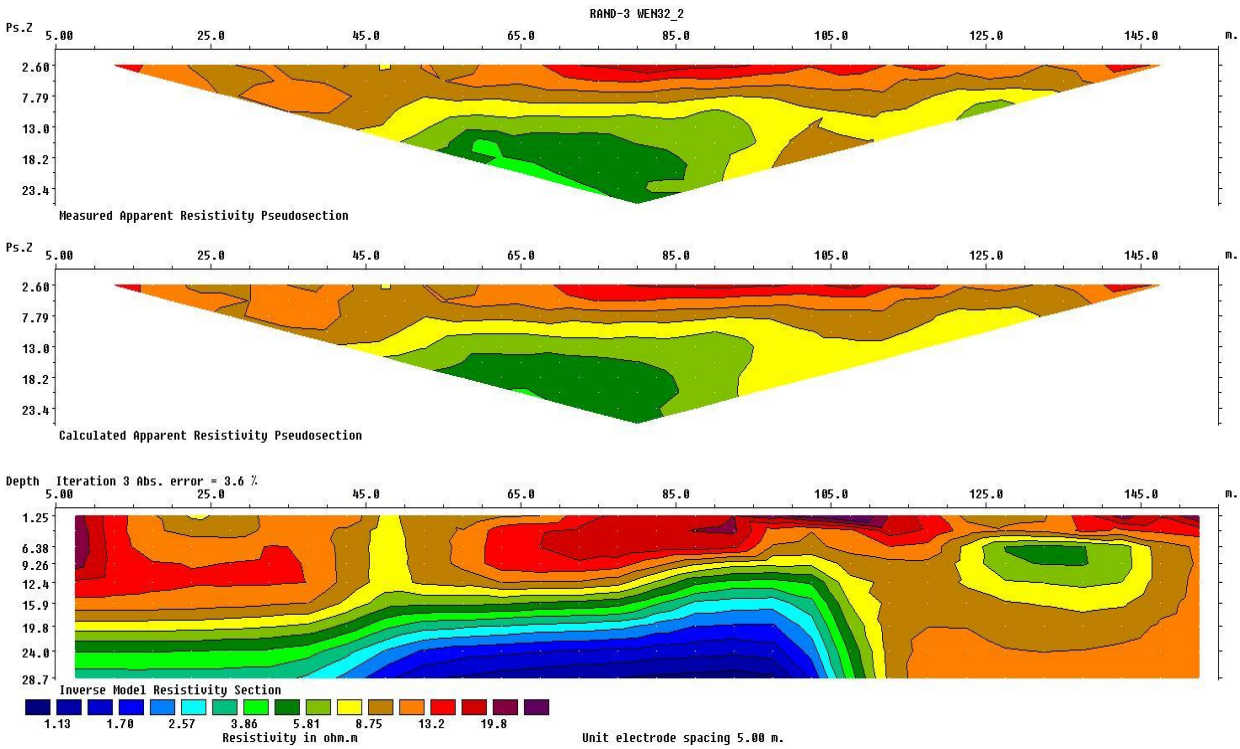

Figure 4. Wenner resistivity section at site E1

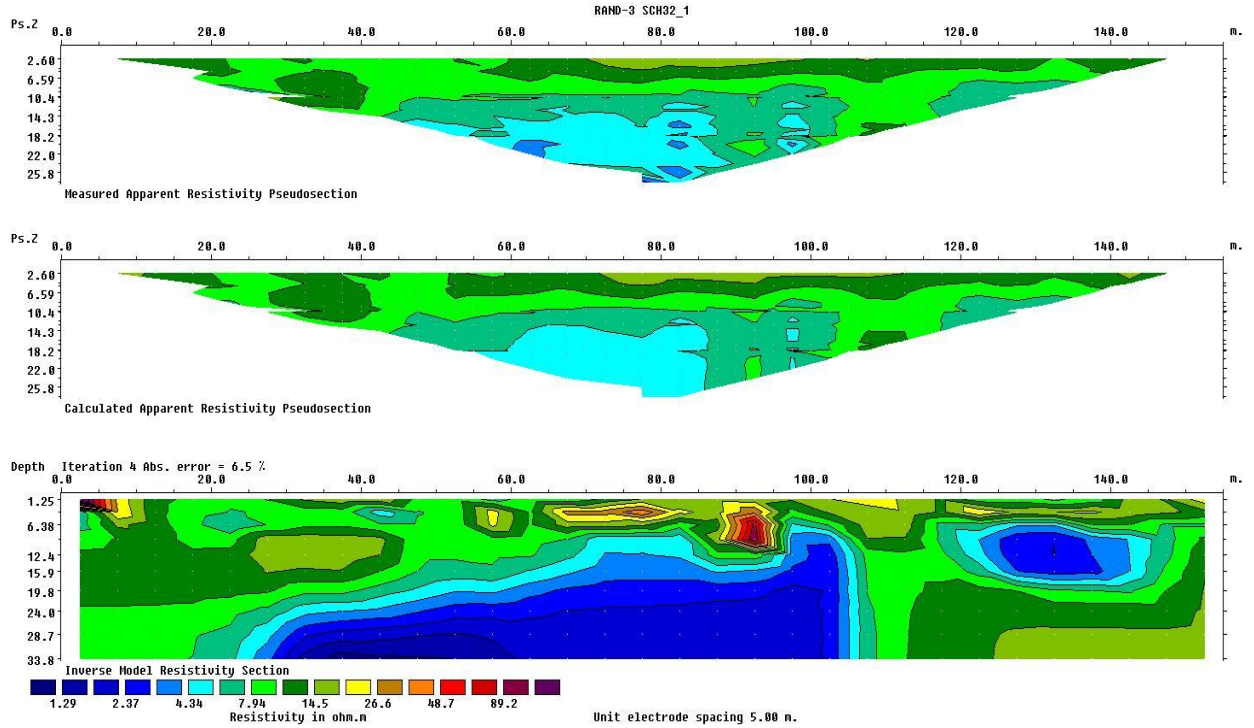

Figure 5. Schlumberger resistivity section at site E1

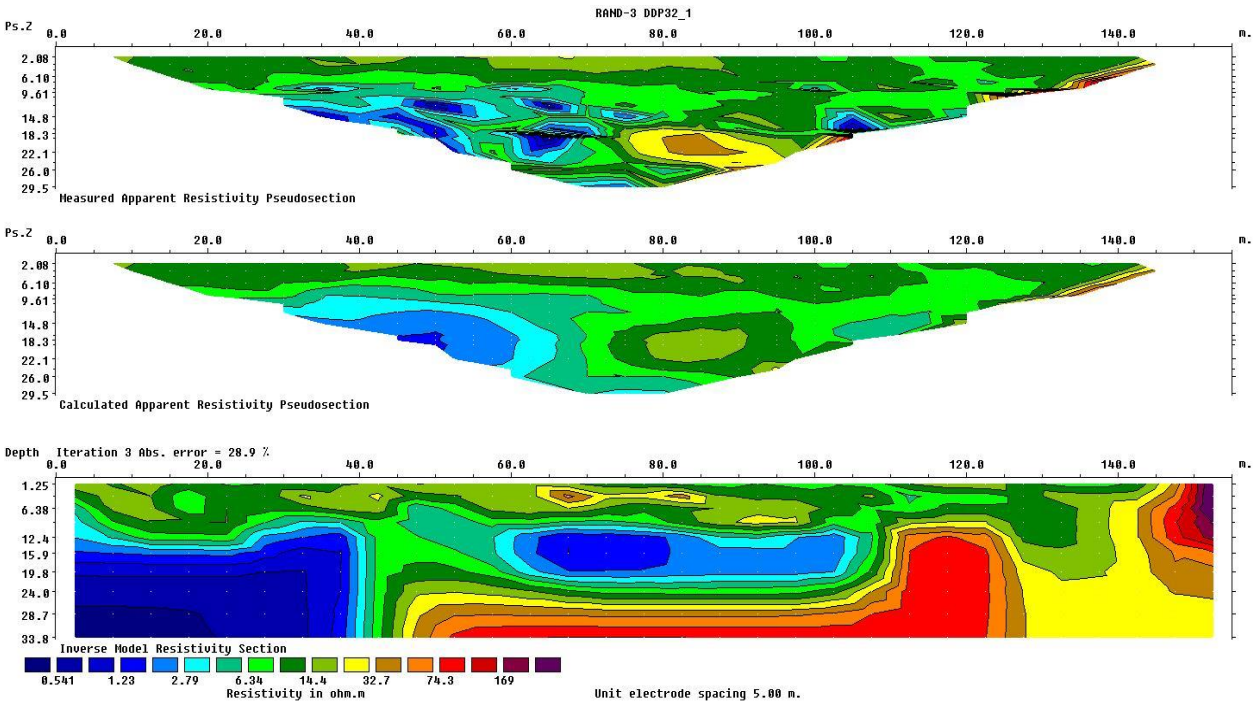

Figure 6. Dipole-Dipole resistivity section at site E1

4.1.1 Correlation with available well data for site E1

The available well near the beginning of Profile E1 gives additional hydrogeological support for interpreting the ERT results. The physicochemical characteristics measured in the well are presented in Table 1. The total well depth is 36 m, with a static water level (SWL) of about 10 m, and a perforation extending from 18 to 36 m. The groundwater exhibits elevated EC (7.62 mS/cm) and TDS (3810 ppm), reflecting mineralized to saline water. All three ERT models indicate low-resistivity areas that may reflect saturated subsurface materials with relatively high-conductivity groundwater. The clearest common conductive feature occupies approximately 55–100 m along the survey line, mainly below about 12m depth. Based on the consistency in all three arrays and supported by the well data, the sector around 65–90 m represents the preferred target for well drilling, with a preferred target depth of about 18–35 m. However, low resistivity can also be influenced by saline groundwater and should not be interpreted as evidence of fresh groundwater. The available well data support the interpretation of the low-resistivity zones as potential saturated areas, whereas the elevated EC and TDS values indicate that saline groundwater plays an important role in the measured low resistivity.

Table 1. Physicochemical characteristics of groundwater from the well at the beginning of profile E1

Total Well Depth (m)	Perforated Interval (m)	SWL (m)	pH	EC (mS/cm)	TDS (ppm)	Groundwater Temperature (°C)	Salinity (%)	Specific Gravity (S.G.)
36	18–36	10	Not Measured	7.62	3810	Not Measured	Not Measured	Not Measured

Note: SWL: Static water level; EC: Electrical conductivity; TDS: Total dissolved solids.

4.2 Profile E2

From Figure 7, the Wenner inversion model indicates a distinct low-resistivity anomaly between about 80 and 140 m, mainly within the 10–20 m depth interval, with some extension to greater depth. This conductive anomaly may represent a possible groundwater-bearing zone. Moderate resistivities prevail in the eastern profile sector, whereas local resistive anomalies are present at shallow depths. The resulting model has an Abs. error of 15.1%, which is suitable for evaluating the main resistivity features.

From Figure 8, the Abs. error of the Schlumberger inversion model is 24.7%, which is due to the heterogeneity of the subsurface. A conductive zone is identified between 40 and 140 m, with a resistivity of less than 4 Ω·m in general. A possible lithological boundary or structural discontinuity is evident at approximately 140–160 m, where there is a sharp resistivity contrast between the conductive and the resistive materials. Immediately east of this boundary, a deep conductive anomaly is observed from 180 to 200 m, which may suggest possible groundwater occurrence.

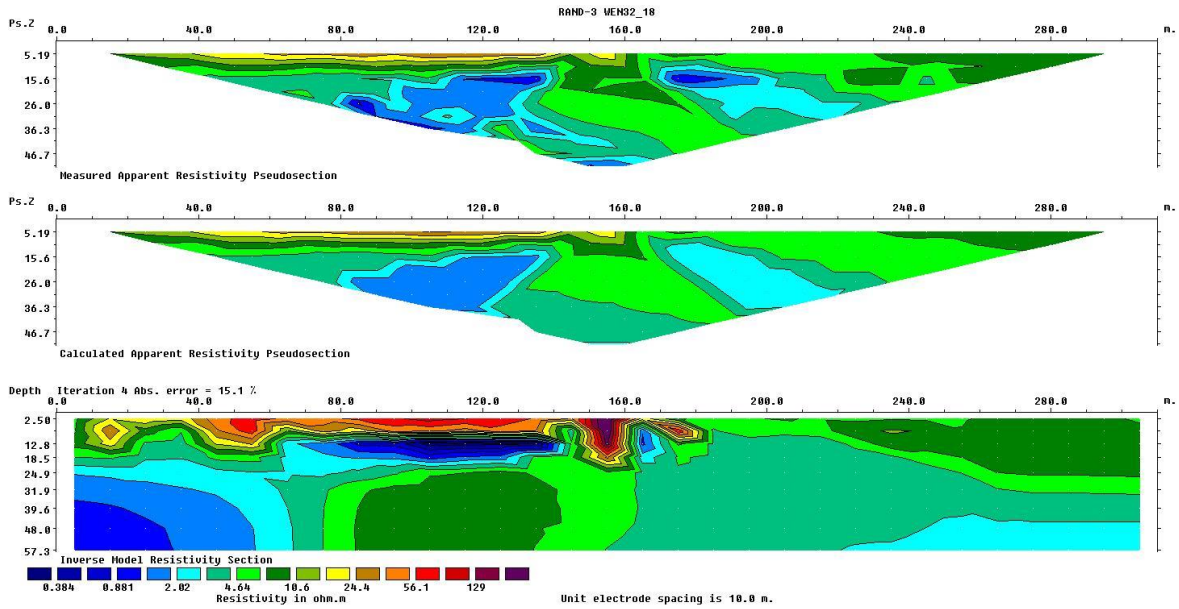

Figure 7. The Wenner resistivity section at site E2

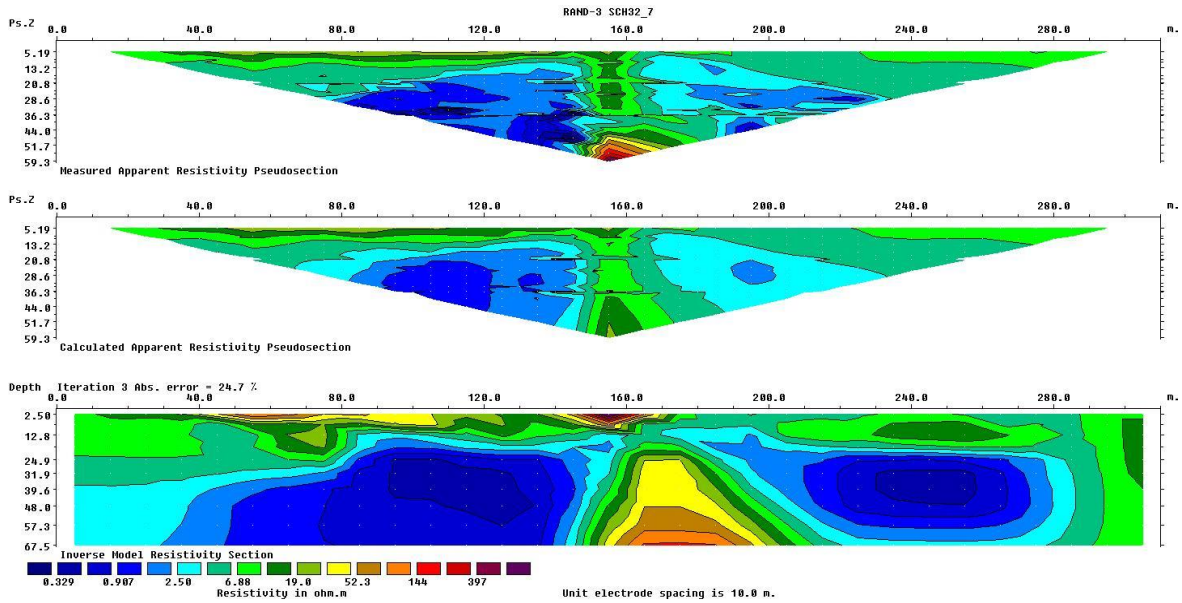

Figure 8. Schlumberger resistivity section at site E2

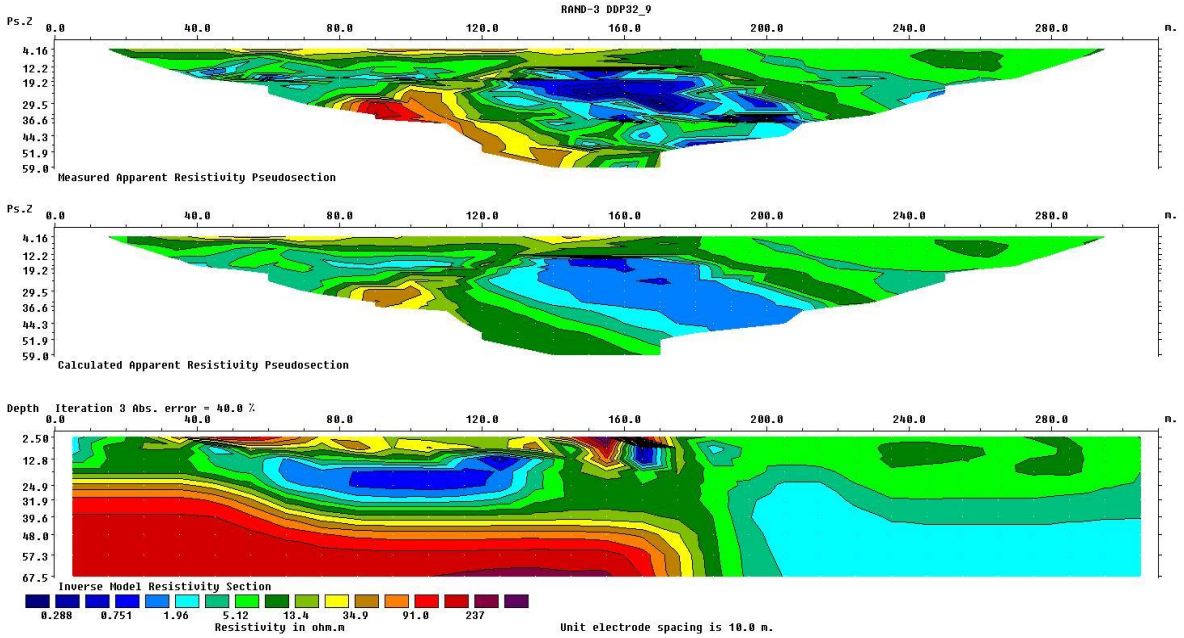

Figure 9. Dipole-Dipole resistivity section at site E2

Table 2. Physicochemical characteristics of groundwater from Well 2

Total Well Depth (m)	Perforated Interval (m)	SWL (m)	pH	EC (mS/cm)	TDS (ppm)	Groundwater Temperature (°C)	Salinity (%)	Specific Gravity (S.G.)
36	18–36	5	7.18	11.55	5770	23	Not measured	Not measured

Note: SWL: Static water level; EC: Electrical conductivity; TDS: Total dissolved solids.

In Figure 9, the Dipole–Dipole section shows a broad conductive zone extending approximately from 40 to 140 m, mainly at shallow to intermediate depths, with resistivity values generally below about 6 Ω·m. In contrast, a large resistive body dominates the deeper western part of the profile, while the eastern sector is characterized by moderate to low resistivity values. The low-resistivity zone may indicate saturated material or saline sediments, while the deep resistive feature may reflect relatively unsaturated or compact sediments. Because the Abs. error is 40%, the interpretation should mainly focus on the broad resistivity pattern rather than minor features.

The three arrays indicate a common conductive zone mainly between about 80 and 140 m along the survey line. The Wenner, Schlumberger, and Dipole–Dipole sections exhibit resistivities of about 0.4–4.6, 0.3–6.9, and 0.3–6.5 Ω·m, respectively, in this interval, within nearly the same area. The consistency among the three arrays indicates that this conductive anomaly may reflect a potential groundwater-bearing zone, especially at depths below about 15–20 m. A second conductive zone is also identified toward the eastern profile sector, especially in the Schlumberger result.

4.2.1 Correlation with available well data for site E2

The nearby well located at the beginning of Profile E2 gives hydrogeological support for the ERT interpretation. The Physicochemical Characteristics of Well 2 can be seen in Table 2. The well has a total depth of 36 m, an SWL of about 5 m, and a perforated interval between 18 and 36 m. The measured EC of 11.55 mS/cm and TDS of 5770 ppm indicate relatively saline and highly conductive groundwater. The three ERT arrays show a common low-resistivity anomaly mainly between about 80 and 140 m along the profile of site 2, with resistivity values generally between 0.4–4.6 Ω·m in the Wenner section, 0.3–6.9 Ω·m in the Schlumberger section, and 0.3–6.5 Ω·m in the Dipole–Dipole section. These conductive zones could reflect saturated sediments, although their very low resistivity is likely enhanced by the relatively high groundwater salinity. Based on the agreement among the three arrays and the nearby well data, the sector between approximately 90 and 130 m is considered the most favorable target for groundwater drilling, particularly within a depth interval of about 18–35 m.

The existing well confirms groundwater occurrence within the investigated depth range, while its high EC and TDS values suggest that groundwater salinity contributes significantly to the low resistivity observed in the ERT sections.

4.3 Profile E3

From Figure 10, the Wenner inversion model is well-matched to the measured data, with an Abs. error of 11.9%. The resistivity is generally below 3 Ω·m in the area between 80 and 140 m along the profile, which may indicate a potential groundwater-bearing condition, and a prominent conductive zone is present. A clear resistive anomaly is seen between 150 and 165 m, which may be a possible hydraulic barrier. Low resistivity may be observed in another conductive zone between 200 and the end of the profile.

In Figure 11, the Abs. error of the Schlumberger inversion model is 17.9%, which is acceptable for the reliability of the model. A broad conductive anomaly is observed in the section from approximately 60 to 140 m and to depths from 15 to more than 50 m. The resistivity values are generally less than 2 Ω·m, which may indicate a thick groundwater-bearing formation. A prominent vertical resistive body is seen near 145–160 m,

which separates the conductive zones and affects the groundwater distribution. There is also a secondary conductive anomaly between 180 and 280 m.

The Dipole–Dipole section shown in Figure 12 reveals a distinct conductive zone between approximately 60 and 150 m at shallow to intermediate depths, with resistivity values generally below about 8 Ω·m. A large resistive body dominates the deeper western part of the profile, while the eastern sector is mainly characterized by moderate resistivity values. The conductive zone may indicate saturated or saline materials, whereas the deeper resistive body may represent relatively dry or possibly compacted deposits. Because the Abs. error is 47.7%, the interpretation should be restricted mainly to the broad resistivity pattern and major subsurface features.

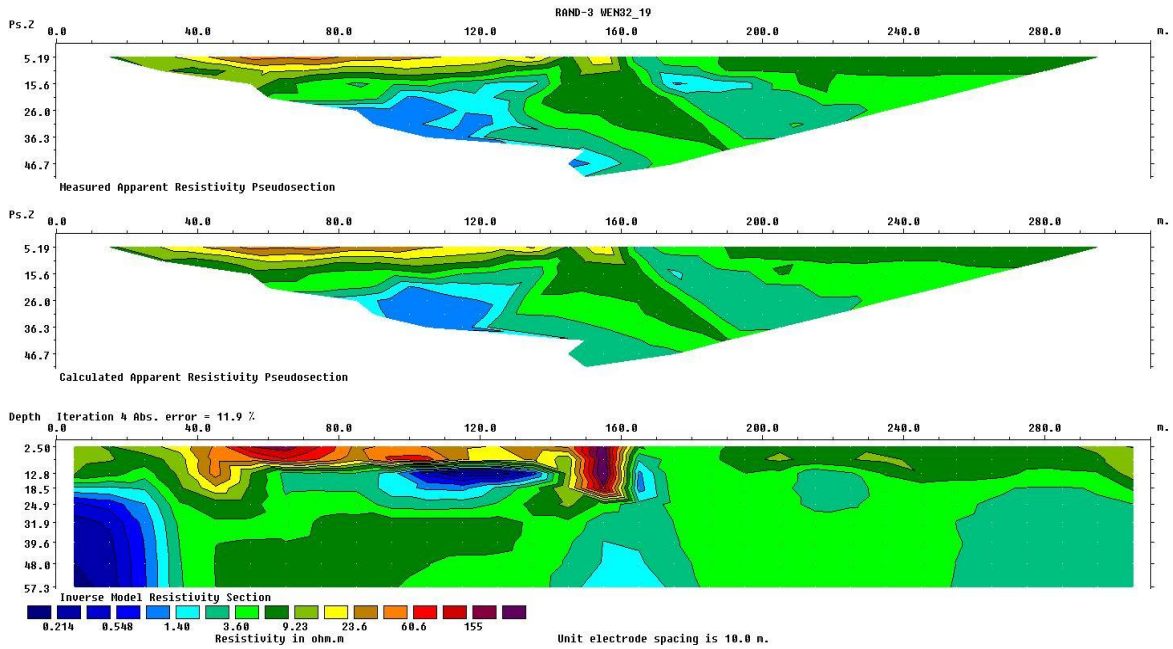

Figure 10. Wenner resistivity section at site E3

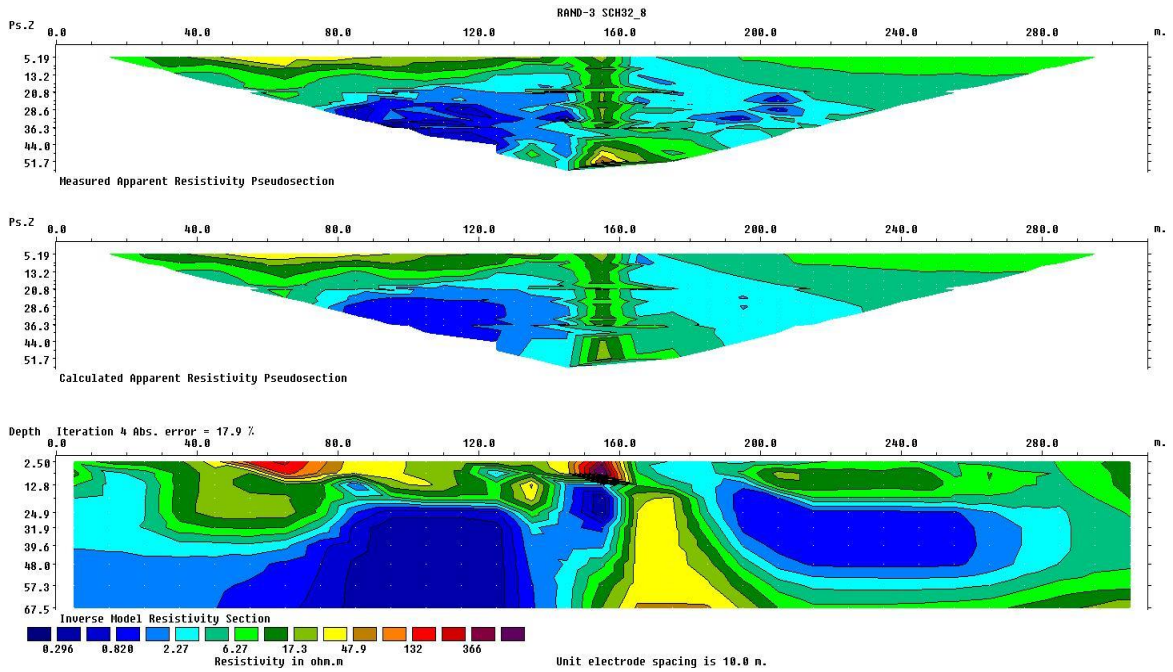

Figure 11. Schlumberger resistivity section at site E3

The three arrays indicate a common low-resistivity zone mainly between approximately 80 and 140 m along the profile. The Wenner, Schlumberger, and Dipole–Dipole sections show resistivity values of approximately 0.2–3.6, 0.3–6.3, and below about 8 Ω·m respectively within this sector, within approximately the same area. The agreement among the three arrays suggests that this conductive zone may represent a possible groundwater exploration target, particularly at depths below about 15–20 m. A second conductive zone is also evident toward the eastern part of the Schlumberger section, although it is less consistently identified by the other arrays.

4.3.1 Correlation with available well data for site E3

The groundwater may be located between the beginning and the middle of Profile E3, which provides useful support for the ERT interpretation, and its physicochemical characteristics can be seen in Table 3. The approximate well depth is 35 m, with a perforated section from 6 to 35 m, and an SWL of about 12 m. The measured EC of 9.81 mS/cm, TDS of 4920 ppm, and salinity of 5040 ppm suggest relatively saline and electrically conductive groundwater. The three ERT arrays reveal a common low-resistivity zone generally between about 80 and 140 m along the profile of site 2, with resistivity values mainly lower than 8 Ω·m. The agreement between this low-resistivity zone and the groundwater characteristics observed in the nearby well supports that the feature may indicate saturated sediments, whereas salinity probably contributes to the low resistivity. Based on the consistency among the three arrays with the available well data, the interval between about 90 and 130 m represents the most favorable sector for groundwater-well installation, especially at depths of about 15–35 m.

The well results therefore provide the interpretation of the main low-resistivity zone as a possible groundwater-bearing feature; however, the low resistivity may be affected by elevated groundwater salinity.

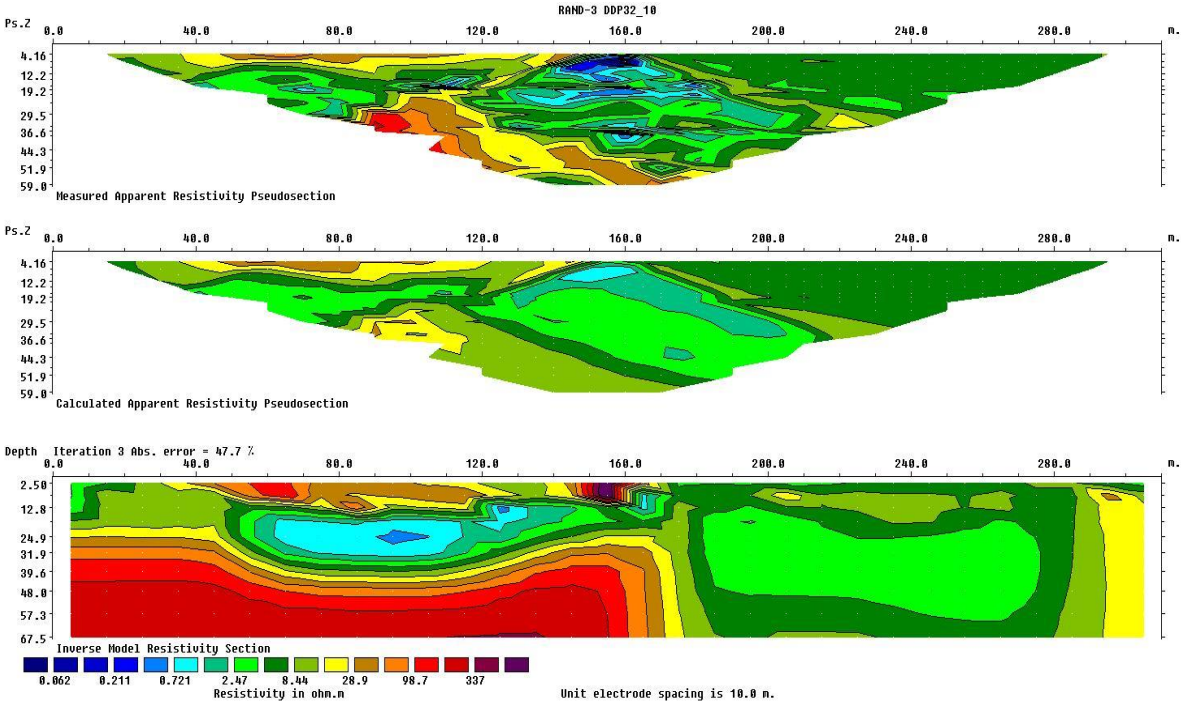

Figure 12. Dipole-Dipole resistivity section at site E3

Table 3. Physicochemical characteristics of the well near profile E3

Total Well Depth (m)	Perforated Interval (m)	SWL (m)	pH	EC (mS/cm)	TDS (ppm)	Groundwater Temperature (°C)	Salinity (%)	Specific Gravity (S.G.)
≈35	6–35	12	7.07	9.81	4920	30	5040	Not measured

Note: SWL: Static water level; EC: Electrical conductivity; TDS: Total dissolved solids.

4.4 Profile E4

As shown in Figure 13, the Wenner inversion result is consistent with the observed data, with an Abs. error of 11.3%. The resistivity section reveals a laterally continuous low-resistivity feature from about 80 to 140 m, with resistivity mainly less than 3 Ω·m, representing saturated deposits and possible groundwater-bearing conditions. A distinct high-resistivity anomaly is observed at about 140–150 m, which is considered a dry boundary or a possible hydraulic barrier. Another conductive zone is also present at the beginning of the profile (0–50 m), but with a lesser lateral extent and thickness than the main conductive zone.

From Figure 14, the Abs. error of the Schlumberger inversion model is 9.2%, which is acceptable for subsurface imaging. The conductive anomaly is wide at depths deeper than 60 m, between approximately 70 and 130 m along the profile. The resistivity values are generally less than 3 Ω·m, which suggests it could be a potential groundwater-bearing formation. A high-resistance body is observed between 140 and 160 m, which could be interpreted as a hydraulic barrier between conductive zones. A secondary conductive anomaly is identified between approximately 190 and 250 m along the profile, which is regarded as a secondary zone that may contain groundwater.

The Wenner and Schlumberger sections show a common low-resistivity zone mainly between approximately 90 and 130 m along the profile. The Wenner section indicates resistivity values of about 1.1–2.8 Ω·m within this sector, whereas the Schlumberger section shows lower values of approximately 0.35–1.9 Ω·m at greater depths. The consistency between the two arrays indicates that this conductive feature may reflect a possible groundwater-bearing condition, generally below about 25 m depth. Another conductive body is shown toward the eastern part of the Schlumberger section.

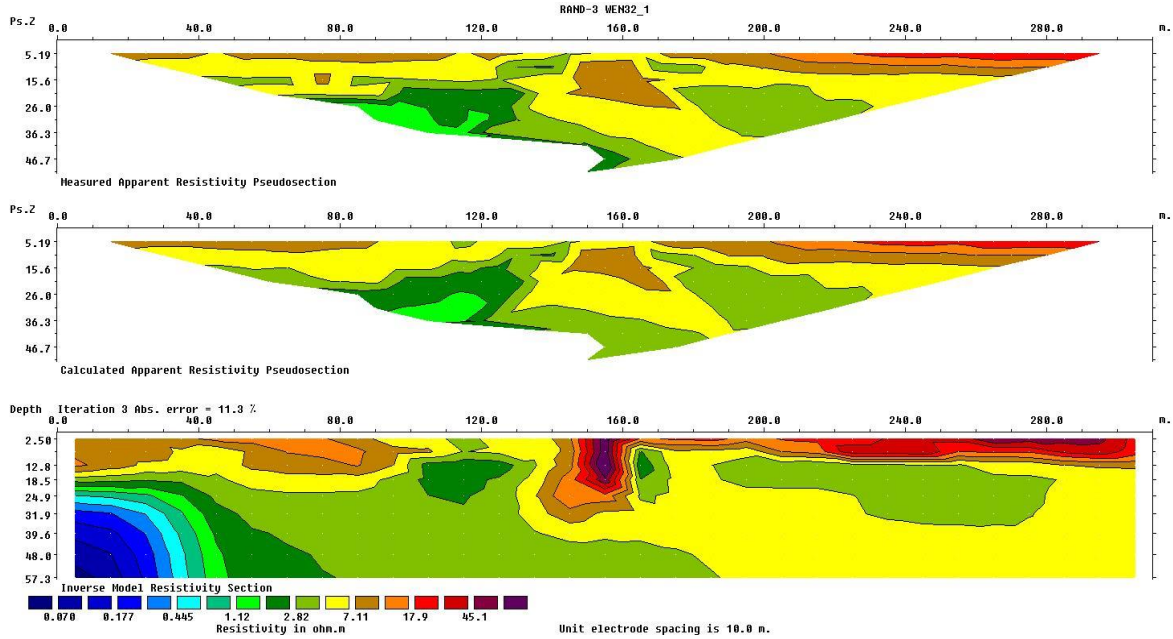

Figure 13. Wenner resistivity section at site E4

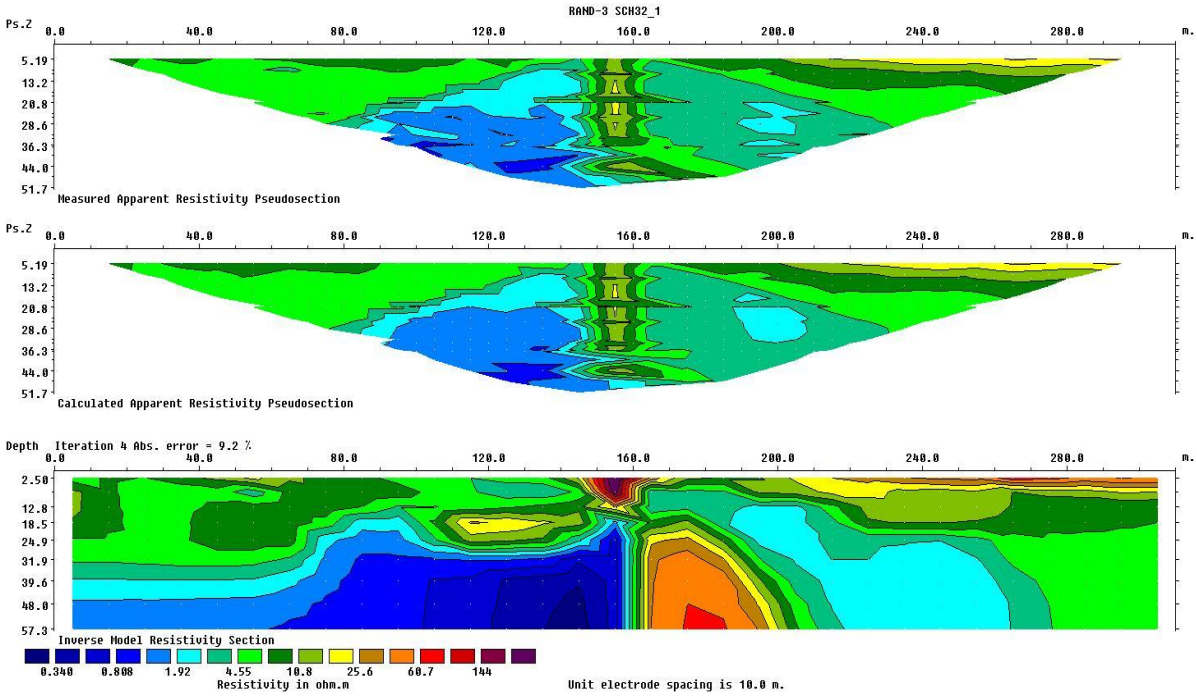

Figure 14. Schlumberger resistivity section at site E4

4.4.1 Correlation with available well data for site E4

The groundwater well located about 90 m from the beginning of Profile E4 offers direct support for the ERT interpretation. Table 4 presents the physicochemical characteristics of Well 4. The well has an approximate total depth of 40 m, a perforated interval between 10–40 m, and an SWL of about 5 m. The measured EC of 6.49 mS/cm, TDS of 3250 ppm, and salinity of 3290 ppm reflect relatively conductive and saline groundwater. The position of the existing well within this conductive feature supports its interpretation as a possible groundwater-bearing zone, whereas the groundwater salinity may contribute generally to the measured low resistivity. Based on both ERT results and well data, the sector between about 95 and 125 m represents the most favorable zone for well drilling, especially within a depth range from 10 to 40 m.

Table 4. Physicochemical characteristics of groundwater from the well near profile E4

Total Well Depth (m)	Perforated Interval (m)	SWL (m)	pH	EC (mS/cm)	TDS (ppm)	Groundwater Temperature (°C)	Salinity (%)	Specific Gravity (S.G.)
≈40	10–40	5	7.00	6.49	3250	Not measured	3290	Not measured

Note: SWL: Static water level; EC: Electrical conductivity; TDS: Total dissolved solids.

4.5 Profile E5

The Wenner inversion model exhibits good agreement between the measured and calculated data, with an absolute Abs. error of 9.1%, as shown in Figure 15. A high-resistivity anomaly is observed in the section from near-surface to deeper depths (150–165 m) with resistivity >600 Ω·m. This is interpreted as a small or cemented feature that may be lithologically impermeable. On the other side of this resistive body, conductive zones are observed with resistivities ranging from 6 to 30 Ω·m. Possible groundwater-bearing zones are those between 100–150 m and 200–280 m, where low resistivity values are noted in saturated sediments and potential groundwater-bearing conditions.

In Figure 16, the Abs. error of the Schlumberger inversion model is 10.9%, which is good for subsurface imaging. The sharp vertical resistivity contrast is observed at a depth of 150–165 m, where conductive materials are found on the west side from 200–280 m that extend to depths of more than 25 m; this feature is known to be a structure that may contain groundwater occurrence. Another conductive zone is observed west of the boundary at approximately 100 and 150 m.

The Dipole–Dipole section exhibits strong lateral and vertical variations in subsurface resistivity, as shown in Figure 17. A pronounced conductive zone occurs mainly between approximately 120 and 170 m at intermediate depths, while a large resistive body dominates the deeper western and central parts of the profile. Toward the eastern part, particularly beyond about 200 m, resistivity decreases markedly at depth. The conductive zones may be associated with saturated or saline materials, whereas the high- resistivity body may represent relatively dry, compact, or coarse deposits. With an Abs. error of 24.7%, the major resistivity features can be considered more reliable than the smaller anomalies.

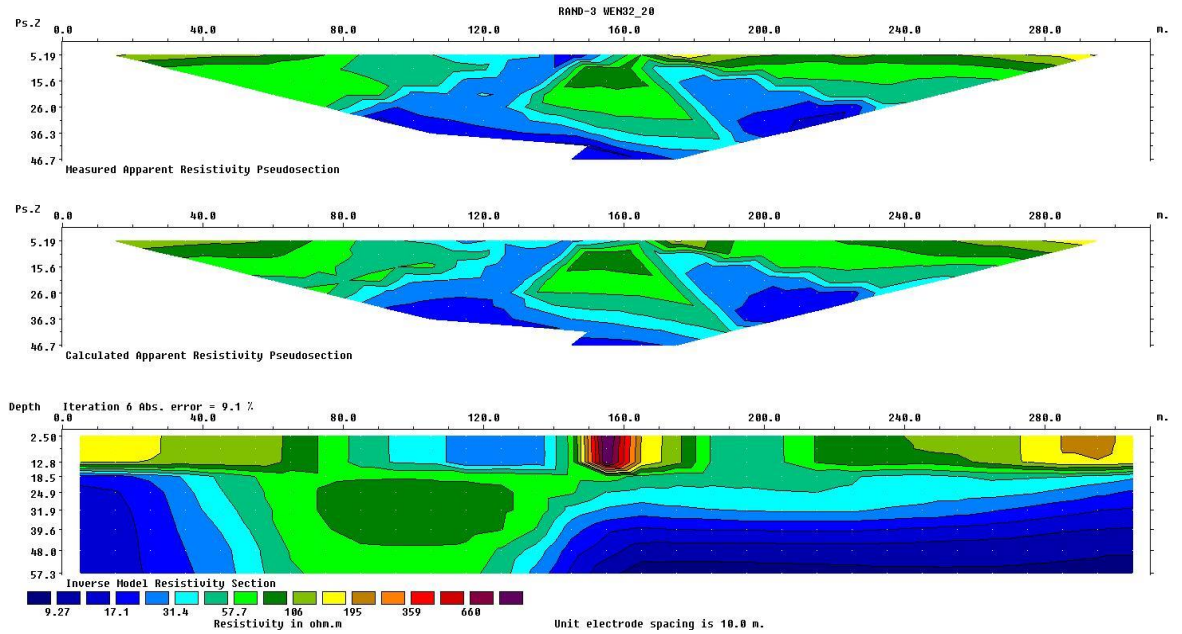

Figure 15. Wenner resistivity section at site E5

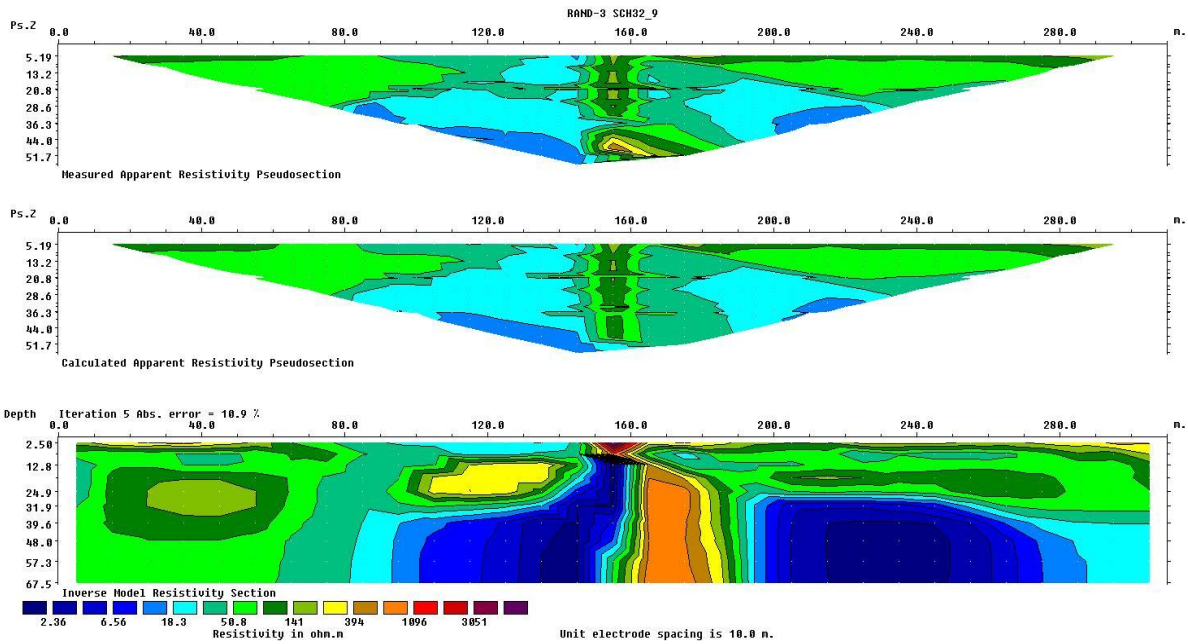

Figure 16. Schlumberger resistivity section at site E5

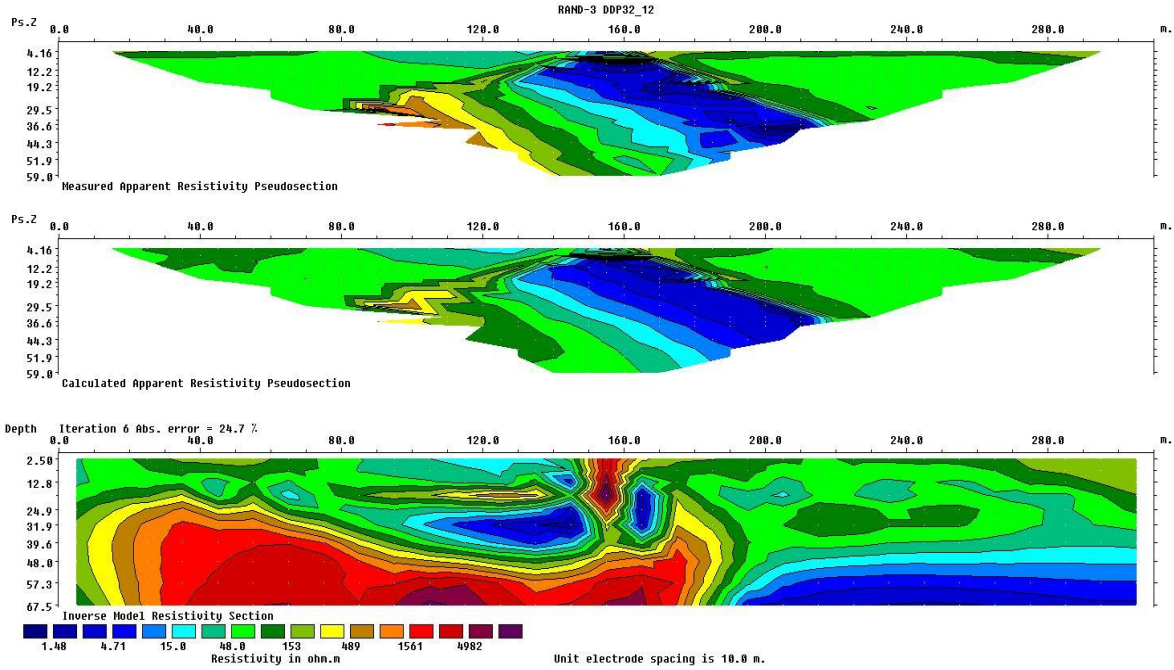

Figure 17. Dipole-Dipole resistivity section at site E5

Table 5. Physicochemical characteristics of the well near profile E5

Total Well Depth (m)	Perforated Interval (m)	SWL (m)	pH	EC (mS/cm)	TDS (ppm)	Groundwater Temperature (°C)	Salinity (%)	Specific Gravity (S.G.)
≈45	Not measured	15	7.25	5.40	2680	Not measured	0.27	1.001

Note: SWL: Static water level; EC: Electrical conductivity; TDS: Total dissolved solids.

The three arrays reveal two main conductive sectors along the profile E5. A relatively localized low-resistivity zone occurs around 120–145 m, whereas a broader and more persistent conductive zone extends approximately between 200 and 270 m, particularly at depths below about 25 m. The Wenner section shows relatively low resistivity values of approximately 9–31 Ω·m within the conductive sectors, while the Schlumberger section indicates values of about 2.4–18 Ω·m. The Dipole–Dipole section also identifies low resistivity values of approximately 1.5–15 Ω·m within the corresponding zones. The agreement among the three arrays suggests that the eastern conductive sector, particularly between about 200 and 270 m, may represent the most potentially saturated zone for groundwater-bearing occurrence.

4.5.1 Correlation with available well data for site E5

The location of the groundwater well is located near the end part of Profile E5 gives useful support for the ERT interpretation. The well has an approximate total depth of 45 m and an SWL of about 15 m. The physicochemical characteristics of the well are listed in Table 5. The measured EC of 5.40 mS/cm and TDS of 2680 ppm indicate relatively conductive and saline groundwater. The three ERT arrays give a large conductive sector toward the eastern part of the survey line, approximately between 200 and 270 m, which continues to deeper levels. The proximity of the existing well to this conductive sector supports its interpretation as a potential groundwater-bearing zone, while the groundwater conductivity may also contribute to the observed low resistivity. Based on the agreement among the ERT arrays and the well data, the sector between approximately 210 and 260 m is considered a favorable target for groundwater drilling, particularly within the depth interval of about 20–45 m.

The nearby well therefore supports the groundwater potential of the eastern conductive zone identified by the three ERT arrays.

4.6 Profile E6

In Figure 18, the Wenner inversion model shows good agreement between the measured and calculated data, with an Abs. error of 5.0%. The section revealed a clear conductive zone (<12 Ω·m) that continues to depths below the western and central parts of the profile from 120 m to the end of the profile, which may reflect the presence of water-saturated sediments, potentially influenced by groundwater salinity and clay content. At about 150–160 m, a vertical resistive anomaly (more than 700 Ω·m) was observed, which is interpreted as a small lithological unit or structural boundary between conductive zones. Towards the eastern part of the profile, a second conductive zone is observed, extending from the beginning of the profile to 50m from it, which represents a second zone that may contain a potential groundwater-bearing accumulation.

In Figure 19, the Abs. error of the Schlumberger inversion model is 18.1%, which is within an acceptable range for the model's reliability. A major resistive body (>1000 Ω·m) is recognized between about 150 and 210 m, extending vertically through the section, and is interpreted as a possible structural feature. On both sides of this anomaly, broad conductive zones (<12 Ω·m) occur between approximately 60–140 m and 200–270 m at depths greater than 25 m. These zones are considered to be saturated formations with a possible groundwater occurrence.

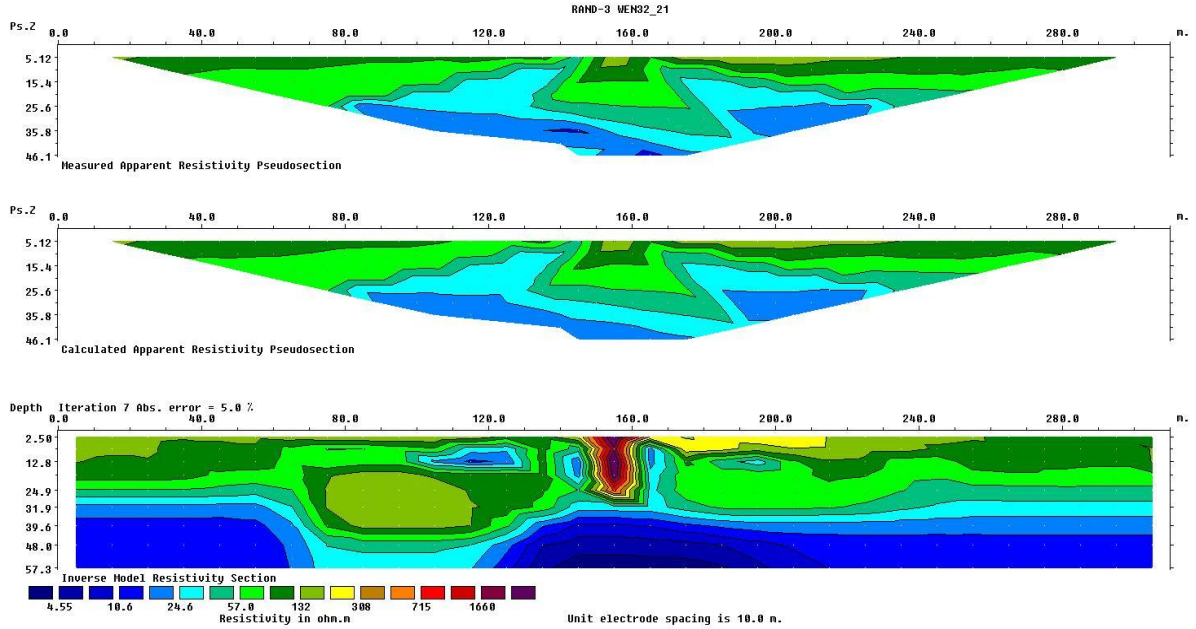

Figure 18. Wenner resistivity section at site E6

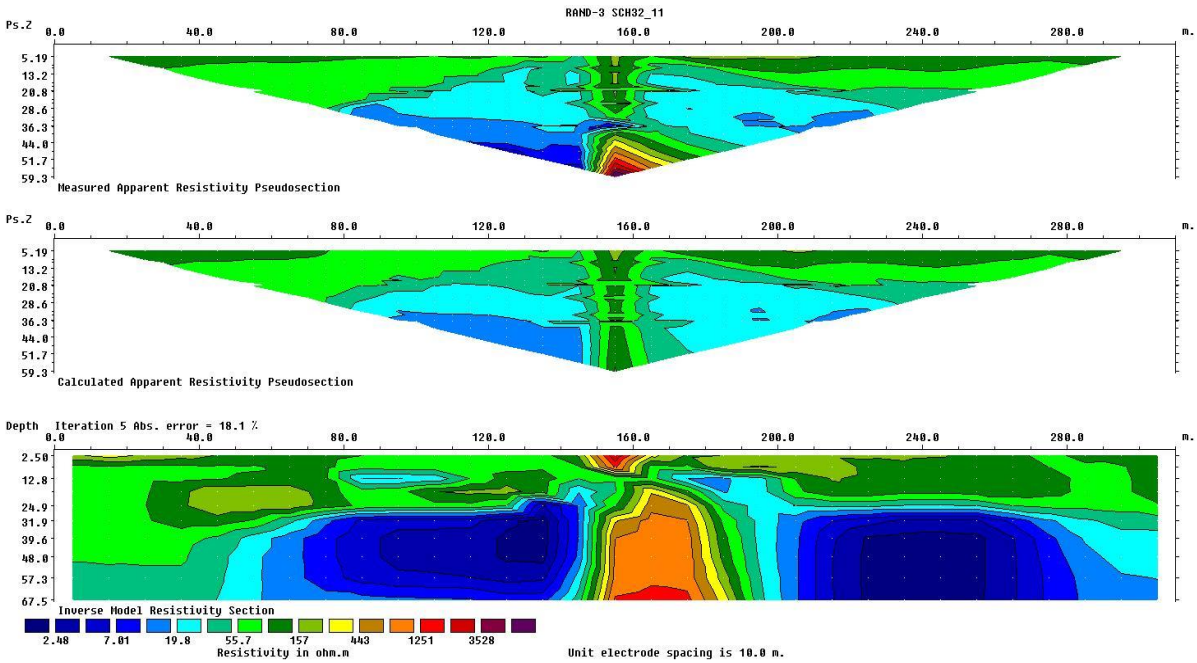

Figure 19. Schlumberger resistivity section at site E6

The Dipole–Dipole section shows strong lateral resistivity variation along the profile as illustrated in Figure 20. A pronounced low-resistivity zone occurs mainly between approximately 110 and 150 m, particularly at depths of about 20–40 m, with resistivity values generally around 0.6–8 Ω·m. This conductive body may indicate water-saturated or saline sediments. In contrast, a broad low-resistivity body dominates the deeper western part of the profile from 200m to the end of the profile, which indicates a possible groundwater-bearing zone. The Abs. error is 22.8%, so the main large-scale features are more reliable than the small localized anomalies.

The three ERT arrays indicate a broad conductive zone toward the eastern part of the profile, particularly between approximately 210 and 270 m. This zone is characterized by relatively low resistivity and extends to depths greater than about 30 m. The agreement among the Wenner, Schlumberger, and Dipole–Dipole sections, with partial support, suggests that the sector around 220–260 m may represent the preliminary borehole target, particularly at depths of approximately 30–50 m below ground level. However, this depth interval represents a preliminary geophysical target rather than a confirmed drilling depth.

4.6.1 Correlation with Available Well Data for site E6

The well located near the end of Profile E6 provides field support for the ERT interpretation. The well has an approximate depth of 45 m and an SWL of about 15 m, confirming groundwater occurrence within the investigated depth range. The measured EC of 5.5 mS/cm and TDS of 2700 ppm indicate relatively conductive groundwater, as illustrated in Table 6. The three ERT arrays identify a persistent conductive zone toward the eastern end of the profile,

approximately between 210 and 270 m. The location of the existing well within this sector supports its interpretation as a potential groundwater-bearing zone. Based on the agreement among the ERT results and the nearby well data, the sector between approximately 220 and 260 m is considered a favorable target for groundwater drilling, particularly within a depth interval of about 30–50 m.

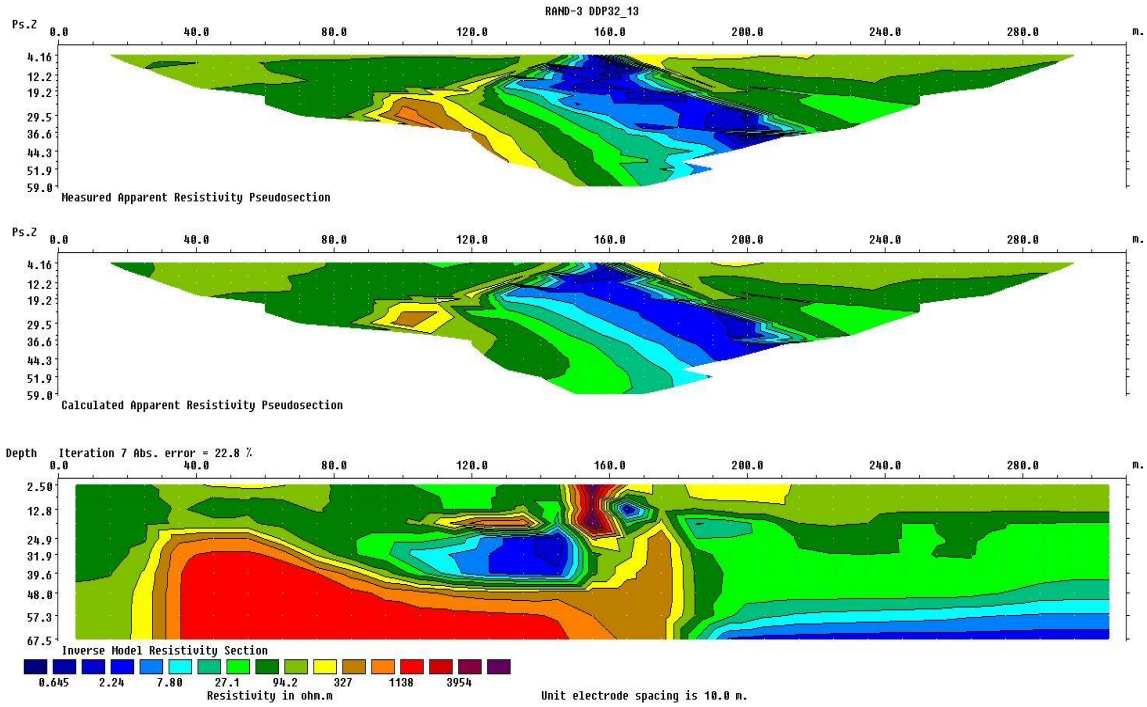

Figure 20. Dipole-Dipole resistivity section at site E6

Table 6. Physicochemical characteristics of the well near profile E6

Total Well Depth (m)	Perforated Interval (m)	SWL (m)	pH	EC (mS/cm)	TDS (ppm)	Groundwater Temperature (°C)	Salinity (%)	Specific Gravity (S.G.)
≈45	Not measured	15	7.30	5.50	2700	Not measured	0.27	1.001

Note: SWL: Static water level; EC: Electrical conductivity; TDS: Total dissolved solids.

4.7 Assessment of inversion models' reliability

The inversion models were assessed by considering their Abs. errors, consistency among electrode arrays, and supporting groundwater well information. The field surveys were carried out under difficult environmental conditions, with temperatures approaching 40 °C during certain measurements. The dry sandy soil also caused poor electrode contact at several locations, resulting in weak or unstable measurements. High contact resistance between electrodes and the ground has been identified as a possible source of measurement errors in previous research [20, 21]. Compared with the Wenner configuration, the Dipole–Dipole array is generally more sensitive to measurement noise but offers improved sensitivity to lateral resistivity changes [22, 23]. Such conditions may partly explain the elevated absolute inversion errors in the Dipole–Dipole sections, especially E1 (28.9%), E2 (40.0%), and E3 (47.7%). Although anomalous data points were excluded during processing, some inverted sections continued to show relatively high error values. Therefore, greater emphasis was placed on the major resistivity features supported by the lower-error arrays and available well data. Small and isolated anomalies in the higher-error models were interpreted cautiously. The proposed drilling targets are considered preliminary and require further field verification.

4.8 Comparative discussion of the six Electrical Resistivity Tomography profiles

The comparison of the six ERT profiles revealed general agreement between the electrode arrays in identifying the main conductive zones, although some differences were observed. All arrays show good consistency in locations of conductive features, except E1, where the Dipole–Dipole anomaly was slightly displaced. Nevertheless, the elevated inversion errors associated with the Dipole–Dipole array, especially in E2 (40.0%) and E3 (47.7%), increase uncertainty in interpreting the finer resistivity features (Table B1, Appendix B). Profiles E5 and E6 generally showed higher resistivity values, with their preliminary target zones occurring at greater depths compared with the remaining profiles. Such differences may be associated with variations in geological materials, groundwater mineralization, and the degree of subsurface saturation. Earlier investigations have reported variations in the ability of different electrode configurations to image subsurface resistivity structures [22, 24]. Accordingly, the consistency among the available arrays provides supporting evidence for the major conductive zones, although the suggested drilling locations still require additional investigation.

5. CONCLUSION

The six ERT profiles showed noticeable changes in subsurface resistivity in both lateral and vertical directions throughout the study area. RES2DINV software was employed to process and invert the acquired measurements, producing resistivity sections for subsurface interpretation.

The 2D ERT surveys were successfully carried out with the Wenner, Schlumberger, and Dipole–Dipole arrays that generally identified the main conductive zones in similar parts of the profiles, although the shape and depth extent varied between arrays.

The low-resistivity anomalies were interpreted as possible groundwater-bearing sectors, especially where the conductive zones were broad, continuous, and recognized in two or more configurations.

The collected well data were consistent with the ERT interpretation because groundwater occurred within depth ranges that generally corresponded to the conductive zones identified in the resistivity sections.

The calculated EC and TDS values showed that the groundwater has generally high EC and salinity. Thus, groundwater salinity is likely one of the major factors contributing to the very low resistivity values identified in several profiles.

The integration of ERT results and well data improved confidence in recognizing the most preferred groundwater features from localized or less reliable zones.

The delineation of the main conductive zones and major subsurface boundaries was in good agreement between the Wenner and Schlumberger arrays; this uniformity increases the confidence in the interpretation and shows the usefulness of using multiple-electrode configurations in groundwater investigations.

Overall, the integration of the three ERT arrays with groundwater well data provided a more reliable approach for identifying potential lithological boundaries and proposing preliminary borehole targets.

The relatively high Abs. errors in some Dipole–Dipole models introduce uncertainty into the interpretation of small-scale resistivity anomalies. Therefore, the proposed borehole targets should be considered preliminary and require further verification through drilling and pumping tests.

The six 2D ERT profiles revealed lateral and vertical variations in subsurface resistivity. The Wenner and Schlumberger arrays generally identified similar conductive zones, while higher inversion errors in some Dipole–Dipole models introduced uncertainty. The integration of ERT results with well data helped identify potential groundwater-bearing zones, although low resistivity may also reflect groundwater salinity or clay-rich sediments. The preliminary borehole targets were identified along E1 at 65–90 m (18–35 m depth), E2 at 90–130 m (18–35 m), E3 at 90–130 m (15–35 m), E4 at 95–125 m (10–40 m), E5 at 210–260 m (20–45 m), and E6 at 220–260 m (30–50 m). These locations represent preliminary targets requiring further verification. Groundwater yield, suitability for drinking or irrigation, and long-term abstraction sustainability have not been established. Therefore, additional drilling investigations, pumping tests, and water quality assessments are required.

REFERENCE

[1] Al-Ansari, N. (2021). Water resources of Iraq. Journal of Earth Sciences and Geotechnical Engineering, 11(2): 15-34. https://doi.org/10.47260/jesge/1122

[2] Al-Ansari, N. (2025). Water resources in Iraq: Perspectives and prognosis. Journal of Water Resources and Geosciences, 4(1): 249-266. https://jwrg.gov.iq/index.php/jwrg/article/view/136.

[3] Loke, M.H. (2015). Tutorial: 2-D and 3-D electrical imaging surveys. Geotomo Software. https://web.gps.caltech.edu/classes/ge111/Docs/ResNotes_Loke.pdf.

[4] Reynolds, J.M. (2011). An Introduction to Applied and Environmental Geophysics. Australian Society of Exploration Geophysicists. Wiley-Blackwell. https://doi.org/10.1071/PVv2011n155other

[5] Law, S.K.H., Sa'don, N.M., Karim, A.R.A. (2026). Integrated geophysical characterization of karst hazards using ERT, SRT, and MASW: A case study from Bau, Sarawak, Malaysia. International Journal of Design & Nature and Ecodynamics, 21(1): 151-162. https://doi.org/10.18280/ijdne.210114

[6] Al-Juboury, A.A., Thabit, J.M., Al-Menshed, F.H. (2019). Determine the groundwater aquifers in southwest of Samawah City (Al Muthanna Governorate), southern Iraq, by using 2-D resistivity imaging survey. Iraqi Journal of Science, 60(4): 792-802.

[7] Al-Hameedawi, M.M., Thabit, J.M., Al-Menshed, F.H. (2022). Integrating geological information and electrical resistivity tomography for mapping the main groundwater-bearing layers in Ancient Babylon City, Iraq. Iraqi Geological Journal, 55(1A): 108-115. https://doi.org/10.46717/igj.55.1A.8Ms-2022-01-27

[8] Noon, M.A., Abed, A.M., Al-Menshed, F.H. (2023). Groundwater investigation using electrical resistivity imaging technique in Western Ramadi, Iraq. Iraqi Geological Journal, 56(2E): 139-145. https://doi.org/10.46717/igj.56.2E.10ms-2023-11-15

[9] Ali, A.A., Al-Khalidy, A.A. (2026). Subsurface soil evaluation using 2D electrical resistivity tomography for foundation studies at Najaf City, Iraq. Iraqi Geological Journal, 59(1C): 134-146. https://doi.org/10.46717/igj.2026.59.1C.10

[10] Zghair, M.M., Al-Kubaisi, M.S., Karim, H.H. (2022). Using 2D electrical resistivity imaging to evaluate soil investigations in Palm Towers site of Al-Muthana Airport, Baghdad, Iraq. Iraqi Geological Journal, 55(2F): 128-137. https://doi.org/10.46717/igj.55.2F.8ms-2022-12-23

[11] Al-Khalidy, A.A., Kadhim, K.N., Al-Tamimi, Q.A., Al-Khafaji, A.J. (2025). Applications of electrical resistivity of soil in design of electrical power station: Case study in Diwaniyah. IOP Conference Series: Earth and Environmental Science, 1545(1): 012006. https://doi.org/10.1088/1755-1315/1545/1/012006

[12] Al-Kubaisi, Q.Y., Aziz, M.K. (2018). Evaluate the climatic conditions for the Karbala. Iraqi Journal of Science, 59(1B): 337-348.

[13] Awadh, S.M., Al-Bahadily, H.A., Al-Ankaz, Z.S. (2018). Interpreting the tectonics of the Abu Jir Fault, Karbala–Najaf Plateau using mineralogical and geophysical data. Iraqi Bulletin of Geology and Mining, 14(1): 47-63.

[14] Loke, M.H. (1999). Electrical imaging surveys for environmental and engineering studies: A practical guide to 2-D and 3-D surveys.

https://pages.mtu.edu/~ctyoung/LOKENOTE.PDF.
[15] Guideline Geo. (2024). ABEM Terrameter LS 2. https://guidelinegeo.com/products/abem/abem-terrameter-ls-2/.
[16] Ali, M.A.H., Mewafy, F.M., Qian, W., et al. (2024). Numerical simulation of geophysical models to detect mining tailings' leachates within tailing storage facilities. Water, 16(5): 753. https://doi.org/10.3390/w16050753
[17] Jaya-Montalvo, M., Jara-Vargas, A., Benavides-Jaramillo, E., Berrezueta, E., Morante-Carballo, F., Carrión-Mero, P. (2025). Application of geophysical methods for the delimitation of potential groundwater zones in rural areas. International Journal of Sustainable Development and Planning, 20(5): 1847-1856. https://doi.org/10.18280/ijsdp.200504
[18] Ohaegbuchu, H.E., Anyadiegwu, F.C., Odoh, P.O., Orji, F.C. (2019). Review of top notch electrode arrays for geoelectrical resistivity surveys. Journal of the Nigerian Society of Physical Sciences, 1(4): 147-155. https://doi.org/10.46481/jnsps.2019.34
[19] Hussein, M.A., Ali, M.Y., Hussein, H.A. (2023). Groundwater investigation through electrical resistivity tomography in the Galhareri district, Galgaduud region, Somalia: Insights into hydrogeological properties. Water, 15(18): 3317. https://doi.org/10.3390/w15183317
[20] Zhou, B., Dahlin, T. (2003). Properties and effects of measurement errors on 2D resistivity imaging surveying. Near Surface Geophysics, 1(3): 105-117. https://doi.org/10.3997/1873-0604.2003001
[21] Carrière, S.D., Chalikakis, K. (2022). Hydrogeophysical monitoring of intense rainfall infiltration in the karst critical zone: A unique electrical resistivity tomography data set. Data in Brief, 40: 107762. https://doi.org/10.1016/j.dib.2021.107762
[22] Dahlin, T., Zhou, B. (2004). A numerical comparison of 2D resistivity imaging with 10 electrode arrays. Geophysical Prospecting, 52(5): 379-398. https://doi.org/10.1111/j.1365-2478.2004.00423.x
[23] Al-Saady, H.A., Karim, H.H., Al-Menshed, F.H. (2022). Comparison of three electrical resistivity arrays to investigate weak zones in soil, along a profile southeast Baghdad City, Iraq. Iraqi Journal of Science, 63(11): 4793-4798. https://doi.org/10.24996/ijs.2022.63.11.18
[24] Moreira, C.A., Montenegro Lapola, M., Carrara, A. (2016). Comparative analyzes among electrical resistivity tomography arrays in the characterization of flow structure in free aquifer. Geofísica Internacional, 55(2): 119-129. https://doi.org/10.22201/igeof.00167169p.2016.55.2.1716

APPENDIX

Appendix A. Electrical Resistivity Tomography field survey parameters

Table A1. Summary of field acquisition parameters and electrode configurations for the six Electrical Resistivity Tomography (ERT) profiles

Profile	Profile Length (m)	Electrode Spacing (m)	No. of Electrodes	Wenner	Schlumberger	Dipole–Dipole
E1	160	5	32	✓	✓	✓
E2	320	10	32	✓	✓	✓
E3	320	10	32	✓	✓	✓
E4	320	10	32	✓	✓	—
E5	320	10	32	✓	✓	✓
E6	320	10	32	✓	✓	✓

Note: ✓ indicates an available dataset used in the analysis; — indicates an array not represented in the final results.

Appendix B. Summary of electrical resistivity tomography inversion results

Table B1. Summary of 2D Electrical Resistivity Tomography (ERT) inversion results for the six survey profiles

Profile	Electrode Array	Iterations	Absolute Error (%)	Model Fit Quality	Resistivity Scale (Ω·m)	Maximum Model Depth (m)
E1	Wenner	3	3.6	High	1.13–19.8	28.7
	Schlumberger	4	6.5	High	1.29–89.2	33.8
	Dipole–Dipole	3	28.9	Low	0.541–169	33.8
E2	Wenner	4	15.1	Moderate	0.384–129	57.3
	Schlumberger	3	24.7	Low	0.329–397	67.5
	Dipole–Dipole	3	40.0	Low	0.288–237	67.5
E3	Wenner	4	11.9	Moderate	0.214–155	57.3
	Schlumberger	4	17.9	Moderate	0.296–366	67.5
	Dipole–Dipole	3	47.7	Low	0.062–337	67.5
E4	Wenner	3	11.3	Moderate	0.070–45.1	57.3
	Schlumberger	4	9.2	High	0.340–144	57.3
E5	Wenner	6	9.1	High	9.27–660	57.3
	Schlumberger	5	10.9	Moderate	2.36–3051	67.5
	Dipole–Dipole	6	24.7	Low	1.48–4982	67.5
E6	Wenner	7	5.0	High	4.55–1660	57.3
	Schlumberger	5	18.1	Moderate	2.48–3528	67.5
	Dipole–Dipole	7	22.8	Low	0.645–3954	67.5

Appendix C. Comparative assessment of Electrical Resistivity Tomography results and preliminary borehole targets

Table C1. Comparative assessment of Electrical Resistivity Tomography (ERT) results and preliminary borehole targets

Profile	Arrays Available	Target Interval (m)	Target Depth (m)	Absolute Error (%) W / S / D–D	Array Consistency	Interpretation Confidence	Remarks
E1	W, S, D–D	65–90	18–35	3.6 / 6.5 / 28.9	2/3 clear; D–D partial	Medium	Good W–S agreement; D–D shows a slight displacement and higher error.
E2	W, S, D–D	90–130	18–35	15.1 / 24.7 / 40.0	2/3	Low	Main conductive zone appears in W and S; high inversion errors limit confidence.
E3	W, S, D–D	90–130	15–35	11.9 / 17.9 / 47.7	2/3	Medium	W–S agreement supports the main conductive zone; D–D interpretation is highly uncertain.
E4	W, S	95–125	10–40	11.3 / 9.2 / N/A	2/2 available	Medium	Agreement between W and S; D–D unavailable due to instrument malfunction.
E5	W, S, D–D	210–260	20–45	9.1 / 10.9 / 24.7	Not established at target	Low	Array agreement at the proposed target requires further verification.
E6	W, S, D–D	220–260	30–50	5.0 / 18.1 / 22.8	2/3; D–D partial	Medium	W–S agreement supports the deeper conductive sector; D–D provides partial support.

Note: W = Wenner; S = Schlumberger; D–D = Dipole–Dipole; N/A = Not available.

A comparative overview of the six investigated ERT profiles, including the proposed borehole target positions and depths, Abs. errors obtained from the inversion model agreement among electrode arrays, and confidence levels assigned to the geophysical investigations is presented in Table C1 in Appendix C.